Mechano-optical waveguide on–off intensity modulator

G. J. Veldhuis, C. Gui, T. Nauta, T. M. Koster, J. W. Berenschot, P. V. Lambeck, J. G. E. Gardeniers, and M. Elwenspoek

MESA Research Institute, University of Twente, P.O. Box 217, NL-7500-AE Enschede, The Netherlands

Received June 9, 1998

High-extinction on–off modulators are essential for channel selection in integrated-optical sensor arrays. We report a standard SiON-technology-based electrostatically driven integrated mechano-optical waveguide on–off intensity modulator. On–off modulation is achieved by movement of an absorbing element into and out of the evanescent field of the guided mode. An extinction ratio of >37 dB at an actuation voltage of <30 V was achieved in a 6 mm × 4 mm device for a wavelength of 632.8 nm. Full wafer-scale fabrication is made possible by use of chemical mechanical polishing and aligned wafer bonding. © 1998 Optical Society of America

OCIS codes: 250.7360, 130.3120.

The field of integrated mechano-optics has been receiving a lot of attention in the past few years.[1] An interesting class in this field is formed by devices that are based on the integrated-optical nanomechanical effect. Here the mechano-optical interaction is obtained by movement of an element into the evanescent field of a guided mode. Figure 1 is a schematic representation of this mechanism. The effect was identified by Lukosz[2] and named after the nanometer-scale movement of the element in the evanescent field, which itself has a penetration depth into the air of the order of the wavelength used (~500 to 1500 nm). A multitude of devices based on the integrated-optical nanomechanical effect have been proposed and demonstrated. Among them are Mach–Zehnder-based 1 × 2 switches,[3,4] Bragg-reflector-based tunable wavelength filters,[4,5] and an acousto-optic sensor.[6] All these devices are essentially based on phase modulation; i.e., a transparent element is moved into the evanescent field, resulting in modulation of the real part of the effective refractive index of the guided mode. In general, the device functionality in these studies was obtained by translation of the phase modulation into an intensity modulation by an interference-based mechanism.

One can also obtain an on–off intensity modulator by electrostatically driving an absorbing element into the evanescent field of the guided mode,[4] which results directly in intensity modulation, since the imaginary part of the effective refractive index of the guided mode is changed. In contrast with a Mach–Zehnder-based modulator, this modulator behavior is nonperiodic, and the extinction that can be obtained is shown to be very high (37 dB). In addition, no actuation is required in the on state. An intrinsic drawback of this approach, however, is the loss of the optical power in the off state, since the mechanism is based on absorption. The device performs an elementary optical function and is expected to be of use in various applications, for example, channel selection in intensity-based integrated-optical sensor arrays,[7] in which high extinction is of major importance.

For an on–off modulator fabricated with sacrificial etching techniques, an extinction ratio of 17 dB for an actuation voltage of 50 V was reported.[4] In this Letter we propose and demonstrate a device that is fabricated through standard silicon technology with a two-wafer technique. The movable elements and the optical waveguides are fabricated separately on mechanical and optical wafers, respectively, and assembled together by use of aligned wafer bonding,[8] which is made possible by chemical mechanical polishing.[9] Owing to good control of the fabrication process, a device with an extinction ratio of 37 dB for a driving voltage of 30 V was obtained. This Letter mainly concerns the device design and performance.

The device is designed with SiON technology for a wavelength of $\lambda = 632.8$ nm (He–Ne) and TE polarization. The waveguide that is used consists of a Si_3N_4 core layer ($n_g = 2.01$) on top of a SiO_2 buffer layer ($n_s = 1.46$). A monomode high-guidance waveguide makes it possible to obtain a large power fraction of the guided mode in the air, while the penetration depth is small.[10] In this way minimal movement of the element is required for obtaining significant effects. The movable element is made of Si ($n_e = 3.85 - 0.019i$), which is not transparent for the wavelength used.

Figure 2 shows the calculated attenuation of the guided slab mode as a function of the gap width between the waveguide and the absorbing element, with core layer thickness d as a parameter. From the

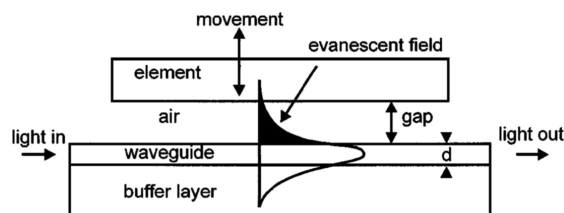

Fig. 1. Schematic representation of the integrated-optical nanomechanical effect.

0146-9592/98/191532-03$15.00/0 © 1998 Optical Society of America

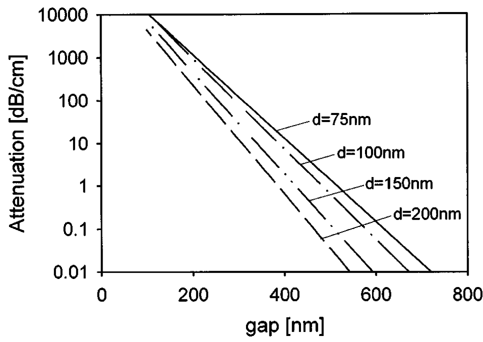

Fig. 2. Attenuation of the guided mode as a function of the gap for different values of the waveguide thickness d.

figure it is clear that for all values of d the effects are extremely large. For example, for a thickness of $d = 200$ nm the attenuation varies over 5 orders of magnitude to more than 1000 dB/cm if the gap width is decreased from 600 to 100 nm. For the reported device $d = 200$ nm was chosen. From the figure it can also be seen that the gap width before actuation has to be larger than 600 nm to ensure that in the on state no significant attenuation (i.e., <0.01 dB/cm) occurs in the modulator. This value, however, cannot be taken as the initial gap width, because the input and output waveguides are covered by a SiO_2 cladding layer ($n = 1.47$) that also serves as a spacer layer in the assembled system. In this region the evanescent field has a larger penetration depth, and the gap width has to be enlarged to 800 nm to ensure that the attenuation is <0.01 dB/cm. Therefore an initial gap width (equal to the cladding thickness) $d_{\mathrm{gap}} = 800$ nm is chosen. The abrupt transition between the SiO_2-clad region of the waveguide and the (air-clad) modulator region is the main source of the insertion loss of the device (i.e., compared with a clad waveguide of the same length). Calculations show that these losses are smaller than 0.05 dB per transition and therefore only 0.1 dB for the complete device. The light is confined laterally by a 2.5-μm-wide, 1.8-nm-high ridge in the Si_3N_4 layer. The thickness of the buffer layer was chosen to be 3 μm, which is sufficient for avoiding losses to the substrate. The resulting waveguide is monomodal. Since most integrated-optical sensors are polarization dependent, the devices were designed for one specific polarization (TE). However, the device behavior is, in principle, polarization independent. Once the absorbing element is down, both TE- and TM-polarized guided light will experience extremely high absorption and reach the off state. Nevertheless, TM polarization will require thicker cladding layers, which will lead to a slight increase in the modulation voltage.

A schematic representation of the membrane and the movable element is given in Fig. 3. The rectangular movable element is located in the center of a four-side clamped rectangular membrane.

The device is actuated electrostatically by application of voltage between the mechanical and the optical silicon wafers. Assuming that the element bending does not contribute to the deflection significantly, the deflection Δ of the element for an actuation voltage V can be calculated[11] from

$$\Delta = \frac{\epsilon_0 V^2 L_p L_o \left(\dfrac{a_p}{2} + \dfrac{a_o}{2}\right)^3}{4({d_{\mathrm{eff}}}^0 - \Delta)^2 E(L_p + L_o){h_m}^3}, \qquad (1)$$

where ϵ_0 is the dielectric constant in vacuum and $E = 160$ GPa is the Young's modulus of single-crystal silicon. The effective distance between the two plates, d_{eff}, can be calculated as $d_{\mathrm{eff}} = d_{\mathrm{gap}}/\epsilon_{r,\mathrm{air}} + d_{\mathrm{Si_3N_4}}/\epsilon_{r,\mathrm{Si_3N_4}} + d_{\mathrm{SiO_2,buffer}}/\epsilon_{r,\mathrm{SiO_2}}$ (see Fig. 1), where $\epsilon_{r,\mathrm{air}} = 1$, $\epsilon_{r,\mathrm{Si_3N_4}} = 4.2$, and $\epsilon_{r,\mathrm{SiO_2}} = 4.4$ are the relative dielectric constants of the materials used.[12] $L_{p,o}$ and $a_{p,o}$ are the length of the element and the membrane, respectively, where the subscript p indicates the dimension in the propagation direction of the light and the subscript o the dimension in the orthogonal direction. The membrane thickness is represented by h_m. To obtain a low actuation voltage one should make the membrane thickness as small as possible. Taking into account technological considerations, $h_m = 30$ μm was chosen. For the technology used the element thickness then equals $h_e = 195$ μm. At a given membrane thickness the voltage required for a given deflection to be obtained decreases as the lateral dimensions of the element and the membrane get larger. For the reported device a compromise between the desired low actuation voltage and small device size was found in the parameters $L_p = L_o = 2$ mm, $a_p = 1.76$ mm, and $a_o = 0.76$ mm. The device size is 6 mm × 4 mm. According to Eq. (1), at $\Delta = 1/3{d_{\mathrm{eff}}}^0$, i.e., when the element is approximately 300 nm above the waveguide, pull-in occurs.[11] This means that in the region 0 nm $< d_{\mathrm{gap}} <$ 300 nm no stable equilibrium for the position of the element exists. If the applied voltage is larger than the pull-in voltage, $V_{\text{pull-in}} = 22.8$ V, the gap will immediately fall to 0 nm, i.e., the position at which the extinction is at maximum. Therefore above 22.8 V the device will switch to the off state.

In the present design the cavity is connected to the outside by air channels defined in the spacer layer. In this way the buildup of air pressure in the chamber, which would result in a higher actuation voltage and more air damping, is avoided.

The device was fabricated as described in Ref. 8. First the extinction was measured as a function of applied voltage V. We eliminated drift effects owing to loading by driving the device by a high-frequency

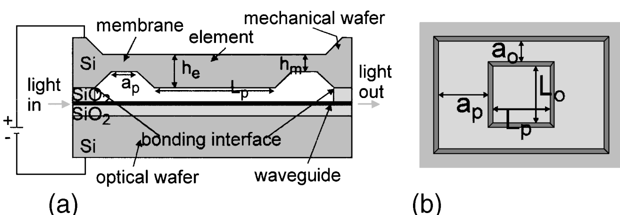

Fig. 3. (a) Length cross section of the presented device and (b) bottom view of the mechanical wafer.

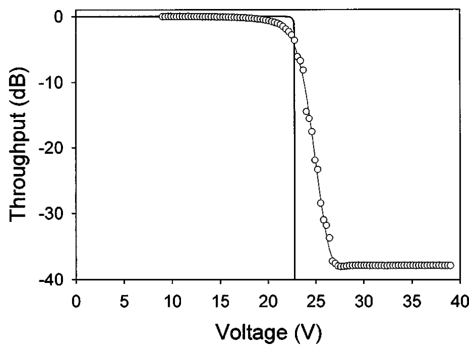

Fig. 4. Throughput versus applied voltage V. The points are the experimentally obtained results. The solid curve is the theoretical behavior.

square voltage.[5] Figure 4 shows the experimental and the theoretical throughput versus the actuation voltage curve, the latter being obtained by combination of the data from Fig. 2 and Eq. (1). In both curves the values of the required driving voltage correspond well to each other. An extinction ratio of 37 dB is obtained for an actuation voltage of 30 V. This is a high extinction ratio value compared with the ratios of 20 dB that are typically obtained by devices based on phase modulation. The real extinction ratio deteriorates as a result of radiation modes that strike the detector, and it is expected that in improved designs, which avoid the occurrence of these modes, even higher extinction ratios will be obtained. The extinction ratio remains constant when the voltage is increased above 30 V. The device shows the intended functionality, and one can use it as an on–off modulator by switching from a voltage below 20 V to a voltage above 30 V. If a throughput attenuation exceeding 0.01 dB/cm is allowed, one can decrease the actuation voltage by choosing a lower value of the initial gap.

Pull-in (i.e., an abrupt increase in the extinction) is not observed in the tested device. This discrepancy between measurement and model is still under investigation, but it is believed that it can be attributed to irregularities in the membrane thickness that cause a nonuniform deflection of the element. Although this behavior was not expected, it permits the use of this device as an analog intensity modulator in which the extinction can be tuned in the range from 0 to 37 dB by application of an appropriate voltage of 20 to 30 V.

The maximum actuation frequency at which the device still shows full extinction is approximately 1 Hz at 30 V. The actuation frequency is limited by damping caused by the air in the gap region.[13] Under vacuum conditions, the fundamental mechanical eigenfrequency of the membrane-element unit was measured to be 17.0 kHz at 20 mTorr, which agrees well with the calculated value of 17.8 kHz.[14] This means that, by sealing the modulator in a vacuum environment in future designs, one can obtain a modulation frequency of at least 1 kHz (which is well below the eigenfrequency).

In conclusion, a new standard SiON-technology-based, electrostatically driven integrated mechano-optical waveguide on–off intensity modulator is reported. An extinction ratio >37 dB at a driving voltage of <30 V has been achieved in a 6-mm-long device for a wavelength of 632.8 nm. Wafer-scale fabrication is made possible by the use of chemical mechanical polishing and aligned wafer bonding. For future designs, several approaches have been proposed to improve further the relevant device characteristics.

A. F. Zwijze is thanked for fruitful discussion. This work was financially supported by the Dutch Innovative Research Program (IOP) Electro-Optics and the Dutch Technology Foundation (STW).

References

1. N. de Rooij and H. Fujita, eds., *1997 IEEE/LEOS, IEEJ/SAMS Conference on Optical Micro Electronic Mechanical Systems* (IEEE, Piscataway, N.J., 1997).
2. W. Lukosz, Proc. SPIE **1793,** 214 (1992).
3. R. Dangel and W. Lukosz, in *Photonics in Switching,* Vol. 10 of OSA Technical Digest Series (Optical Society of America, Washington, D.C., 1997), p. 170.
4. G. A. Magel, Proc. SPIE **2686,** 54 (1996).
5. W. Gabathuler and W. Lukosz, Opt. Commun. **145,** 258 (1998).
6. P. Pliska and W. Lukosz, Sensors Actuators A **41–42,** 93 (1994).
7. G. J. Veldhuis and P. V. Lambeck, Appl. Phys. Lett. **71,** 2895 (1997).
8. C. Gui, G. J. Veldhuis, T. M. Koster, P. V. Lambeck, J. W. Berenschot, J. G. E. Gardeniers, and M. Elwenspoek, in *Proceedings of the 1998 IEEE Workshop on Micro Electro Mechanical Systems* (IEEE, Piscataway, N.J., 1998), p. 482.
9. C. Gui, H. Albers, J. G. E. Gardeniers, M. Elwenspoek, and P. V. Lambeck, Res. J. Microsyst. Technol. **3,** 122 (1997).
10. O. Parriaux and G. J. Veldhuis, J. Lightwave Technol. **16,** 573 (1998).
11. S. P. Timoshenko and S. Woinowsky-Krieger, *Theory of Plates and Shells,* 2nd ed. (McGraw-Hill, New York, 1959).
12. D. R. Lide, ed., *Handbook of Chemistry and Physics* (CRC, Boca Raton, Fla., 1997).
13. H. Hosaka, K. Itao, and S. Kuroda, Sensors Actuators A **49,** 87 (1995).
14. U. Gösele, H. Stenzel, T. Martini, J. Steinkirchner, D. Conrad, and K. Scheerschmidt, Appl. Phys. Lett. **67,** 3614 (1995).